ANTIMICROBIAL AGENTS AND CHEMOTHERAPY, Apr. 2005, p. 1502–1508 Vol. 49, No. 4
0066-4804/05/$08.00+0 doi:10.1128/AAC.49.4.1502–1508.2005

Efficacy of Ciprofloxacin-Releasing Bioabsorbable Osteoconductive Bone Defect Filler for Treatment of Experimental Osteomyelitis Due to *Staphylococcus aureus*

Jyri K. Koort,[1]† Tatu J. Mäkinen,[1]† Esa Suokas,[2] Minna Veiranto,[2] Jari Jalava,[3] Juhani Knuuti,[4] Pertti Törmälä,[2] and Hannu T. Aro[1]*

Orthopaedic Research Unit, Department of Orthopaedic Surgery and Traumatology,[1] and Turku PET Centre,[4] University of Turku, and Department of Human Microbial Ecology and Inflammation, National Public Health Institute,[3] Turku, and Institute of Biomaterials, Tampere University of Technology, Tampere,[2] Finland

Received 22 June 2004/Returned for modification 11 October 2004/Accepted 8 December 2004

The concept of local antibiotic delivery via biodegradable bone defect fillers with multifunctional properties for the treatment of bone infections is highly appealing. Fillers can be used to obliterate surgical dead space and to provide targeted local bactericidal concentrations in tissue for extended periods. Eventually, the osteoconductive component of the filler could guide the healing of the bone defect. The present experimental study was carried out to test this concept in a localized *Staphylococcus aureus* osteomyelitis model in the rabbit ($n = 31$). A metaphyseal defect of the tibia was filled with a block of bone cement, followed by insertion of a bacterial inoculum. After removal of the bone cement and surgical debridement at 2 weeks, the defect was filled with a ciprofloxacin-containing (7.6% ± 0.1%, by weight) composite (treated-infection group) or with a composite without antibiotic (sham-treated group). Both a positive control group (untreated-infection group) and a negative control group were also produced. The treatment response, monitored by positron emission tomography (PET) with fluorine-18-labeled fluorodeoxyglucose ([^{18}F]FDG) at 3 and 6 weeks, showed rapidly decreasing amounts of [^{18}F]FDG uptake in the treated-infection group ($P = 0.001$ compared with the results for the untreated-infection group at 6 weeks). The bacteriological analysis confirmed the eradication of the bone pathogen in the treated-infection group. However, three animals had culture-positive soft tissue infections. All animals in the sham-treated and untreated-infection groups had culture-positive bone infections with typical radiographic changes of osteomyelitis. Histomorphometry, peripheral quantitative computed tomography, and backscattered electron imaging of scanning electron microscopy images verified the osteoconductive properties of the bioactive glass microspheres within the composite. The median bone ciprofloxacin concentrations were 1.2 and 2.1 μg/g at two anatomic locations of the tibia. This is the first report to show the value of [^{18}F]FDG PET for quantitative monitoring of the treatment response in bone infections. The collaborative results of bacteriologic and [^{18}F-FDG] PET studies showed that use of the multifunctional composite was successful for eradication of the *S. aureus* pathogen from bone.

Treatment of osteomyelitis in adults is based on a systematic approach (3, 40), starting from the accurate identification of the pathogen and its sensitivity to antimicrobial treatment. The treatment keystones are radical surgical debridement of the infected tissues, obliteration of the dead space, adequate soft tissue coverage, and a minimum of 4 to 6 weeks of intravenous antimicrobial therapy (3, 35). However, there are still significant relapse rates, even with such vigorous treatment programs; and therefore, alternative strategies have been introduced.

Recently, several local drug delivery systems with bioabsorbable materials have been studied in vitro (17) and in vivo (2). Limited clinical reports are also available (26), but the U.S. Food and Drug Administration has not yet approved the use of any of these materials for antimicrobial therapy (11). Biodegradable implants could provide high local bactericidal concentrations in tissue for the prolonged time needed to completely eradicate the infection and the possibility to match the rate of implant biodegradability according to the type of infection treated (18). Biodegradation also makes surgical removal of the implant unnecessary. The implant can also be used initially to obliterate the dead space and, eventually, to guide its repair.

Thus, there is a place for the development of a new type of bioabsorbable implants with multifunctional properties. We have studied a new drug delivery system based on controlled ciprofloxacin release from a bioabsorbable polylactide matrix with an osteoconductive component. This type of bone defect filler with antimicrobial properties could restore the bone stock after the successful eradication of an infection. The present study was designed to examine the efficacy of the multifunctional bioabsorbable implant for the treatment of experimental osteomyelitis. The treatment response was followed by positron emission tomography (PET) with [^{18}F]fluorodeoxyglucose ([^{18}F]FDG).

* Corresponding author. Mailing address: Orthopaedic Research Unit, Department of Orthopaedic Surgery and Traumatology, University of Turku, FIN-20520 Turku, Finland. Phone: 358-2-313 0000 (hospital) or 358-40-514 4149 (mobile). Fax: 358-2-313 2284. E-mail: hannu.aro@utu.fi.

† J.K.K. and T.J.M. contributed equally to this work.

MATERIALS AND METHODS

Biomaterial. The biomaterial consisted of three components. The matrix was bioabsorbable racemic poly(DL)-lactide (PDLLA; 50:50; Resomer R206; Boehringer Ingelheim, Ingelheim, Germany) with an average molecular mass of

138,000 g/mol. The selected antibiotic (AB) was ciprofloxacin (purchased from Jinxing Kangle Pharmaceutical Factory, Zhejiang, China). According to the quality certificates provided by the manufacturer, the quality of ciprofloxacin was tested as directed in USP23 specifications. Microspheres of a bioactive glass (BaG; glass 13-93), purchased from Vivoxid Ltd., Turku, Finland, were added to act as the osteoconductive component in order to promote new bone formation. The biomaterial was manufactured by compounding the vacuum-dried components by melting in a small laboratory-scale mixer. The melting temperatures used for compounding (~150°C) were much lower than the measured melting point of ciprofloxacin (270°C). The thermal stability of ciprofloxacin was ensured by differential scanning calorimetry before and after compounding. In addition, the bactericidal activity of the compounded ciprofloxacin was proved in separate tests and was compared with the activity of nonprocessed ciprofloxacin. The compounded strands were cut into pellet form. The geometry of the pellets was cylindrical, with an average diameter of 1.0 mm and a length of 0.9 mm. The pellets were sterilized with γ irradiation with a nominal dose of 25 kGy (Willy Rüsch AG, Kernen-Rommelshausen, Germany).

Ciprofloxacin content, release, and antimicrobial activity in vitro. The initial ciprofloxacin content measured in the pellets was 7.6% ± 0.1% (by weight). Detailed in vitro studies were carried out to delineate the release characteristics of the composite and to verify the antimicrobial activity of the released ciprofloxacin at all stages of composite degradation. The concentration of ciprofloxacin released from the PDLLA pellets (500 mg) was measured as a function of the in vitro immersion time in phosphate buffer solution. After the initial burst (36.6 μg/ml/day) on the first day of immersion, the concentration of ciprofloxacin remained at the therapeutic level (>2 μg/ml) but stayed below the level (20 μg/ml) that has been shown to inhibit the proliferation of human osteoblast-like cells in vitro (27) throughout the first 300 days (J. K. Koort, E. Suokas, M. Veiranto, J. Jalava, P. Törmälä, and H. T. Aro, unpublished data). On the basis of testing of the MICs for common bone pathogens (*Staphylococcus aureus*, *Pseudomonas aeruginosa*, *Staphylococcus epidermidis*, and *Escherichia coli*), the bactericidal activity of the released antibiotic remained the same as that of normal ciprofloxacin throughout the manufacturing and sterilization processes and also during the sustained release in vitro (Koort et al., unpublished).

Experimental model of osteomyelitis. The localized osteomyelitis model (stage IIIA of the Cierny-Mader classification [3]) was modified from the canine model of Fitzgerald (7). The results of a part of this study (the results for the untreated-infection and negative control groups) were reported previously (21) in an effort to explore the usefulness of PET for use in the diagnosis of osteomyelitis. Surgery was performed on adult male New Zealand White rabbits ($n = 31$; mean weight, 2,876 g; weight range, 2,532 to 3,505 g; standard deviation [SD], 212 g; Harlan, Horst, The Netherlands). The Ethical Committee of the University of Turku and the Provincial State Office of Western Finland approved the study protocol. All experiments were carried out in accordance with the guidelines of the local Animal Welfare Committee.

The study was preceded by a pilot study ($n = 12$) for optimization of the inoculation dose of *S. aureus* required for the induction of stage IIIA osteomyelitis in the rabbit tibia. In the pilot study, the animals were inoculated with doses (10^4 to 10^7 CFU/ml) of *S. aureus* that were decreased in a stepwise fashion in order to find the optimal dose. In the final experiment, a dose of 0.1 ml of 10^5 CFU of *S. aureus* (strain 52/52A/80) per ml was selected and was found to constantly induce local osteomyelitis (33).

The animals were premedicated by subcutaneous injection of 1 mg of atropine (Atropin; Oy Leiras Ab, Turku, Finland) per kg of body weight, and anesthesia was induced by subcutaneous injection of 0.3 ml of fentanyl citrate-fluanisone (Hypnorm; 0.315 mg of fentanyl citrate per ml and 10 mg of fluanisone per ml; Janssen Pharmaceutica, Beerse, Belgium) per kg and was supplemented by another dose (0.2 to 0.4 ml of fentanyl citrate-fluanisone per kg), if necessary. By using sterile surgical conditions, a cortical bone window (6 by 2.7 mm) was drilled under saline cooling into the proximal medial metaphysis of the right tibia. The local bone marrow was removed by saline lavage, and the defect created in the medullary cavity was filled with a small block of polymerized bone cement (Palacos R-40; Schering-Plough Europe). Bone cement was applied to act as foreign body for intramedullary infection. The periosteal and fascial layers were closed over the cortical defect, and 0.1 ml of 10^5 CFU of *S. aureus* (strain 52/52A/80; kindly provided by Jon T. Mader) per ml was injected into the medullary space surrounding the bone cement. Finally, the skin wound was closed in layers and an intramuscular injection of 0.1 mg of naloxone (Narcanti; Bristol-Myers Squibb S.p.A., Anagni, Italy) per ml was given. Infection was allowed to develop for 2 weeks, when the animals underwent second-stage surgery. By using the previous surgical approach, the defect area was exposed and swab specimens for culture were taken in order to confirm the clinical success of the induction of staphylococcal bone infection. The swab specimens were cultured for 20 h at 35°C on blood agar plates. The bone cement was removed and separately cultured for 4 days at 35°C in brain heart infusion (BBL, Becton Dickinson Microbiology Systems, Cockeysville, Md.) solution. The defect space was lavaged with saline. Any soft tissue with necrosis was surgically excised. In the treated-infection group ($n = 9$), the antibiotic-containing composite (AB-PDLLA-BaG) was then impacted into the medullary space to treat the infection. The wound was closed in layers. Three separate groups of control animals were produced. In the untreated-infection group ($n = 8$), the infected medullary space was left untreated after removal of the cement block and necrotic tissues. In the sham-treated group ($n = 5$), the infected medullary space was filled with a composite without antibiotic (PDLLA-BaG). In one additional control animal, the infected medullary space was filled with BaG microspheres only. In the negative control group ($n = 8$), the bacterial suspension was replaced by saline (0.1 ml) during bone cement application. At 2 weeks, the cement block was removed as for the other groups and the bone was left to heal without any intervention. In the negative control group, a single prophylactic dose of 500,000 IU of benzylpenicillin (Geepenil; Orion Oyj, Espoo, Finland) was given intramuscularly before surgery. In the other groups, no prophylactic antibiotics were given during the surgical procedures. The animals were closely monitored after surgery. Functional activity was not limited. The animals received standard postoperative pain medication (carprofen; 4 mg/kg; Rimadyl Vet; Pfizer, Vericore Ltd., Dundee, United Kingdom) for 3 days.

[^{18}F]FDG PET imaging. The use of [^{18}F]FDG PET to image bacterial infections is based on the intensive use of glucose by granulocytes and mononuclear cells (37). In the present study, the method was applied to monitor the treatment response. [^{18}F]FDG PET imaging of each animal was performed 3 and 6 weeks after the second-stage surgery. PET imaging had been performed with four animals before surgery in order to confirm the equal uptake of the tracer by the intact right and left tibias. [^{18}F]FDG PET imaging was performed as described previously (21). For imaging, the animals were sedated by a subcutaneous injection of 0.3 ml of fentanyl citrate-fluanisone (Hypnorm; 0.315 mg of fentanyl citrate per ml and 10 mg of fluanisone per ml; Janssen Pharmaceutica) per kg. A mean of 94 MBq of [^{18}F]FDG (range, 46 to 121 MBq) was injected in the ear artery of the rabbit. PET was performed by using an Advanced Whole-Body PET scanner (General Electric Medical Systems, Milwaukee, Wis.), which acquires 35 contiguous slices with an axial field of view of 15.2 cm (4). Data were corrected for dead time, decay, and photon attenuation; and the images were reconstructed in a matrix of 128 by 128 pixels. Quantitative analysis was performed for standardized circular regions of interest (ROI; radius, 3.8 mm) of the defect area of the right tibia and the corresponding region of the contralateral intact left tibia. The average radioactivity concentration in an ROI was used for the comparative analysis of the two sides. The levels of [^{18}F]FDG accumulation were reported as the standardized uptake value (SUV). The SUV was calculated as the radioactivity of the ROI divided by the relative injected dose expressed per kilogram of body weight. In addition, SUV ratios between the operated and the nonoperated sides were calculated. During the PET image analysis, the peripheral quantitative computed tomography (pQCT) image of each bone was used as the reference for the constant anatomic positioning of the ROIs.

pQCT. Aside from [^{18}F]FDG PET imaging, each animal underwent pQCT imaging 3 and 6 weeks after the second-stage surgery. With the animal under sedation, the right hind limb was placed in a holder and imaged with a Stratec XCT Research M pQCT device (Norland Stratec Medizintechnik GmbH, Birkenfeld, Germany). After an initial scouting view, scanning of the bone defect was performed in the horizontal plane with the use of six consecutive cross-sectional images with a slice distance of 0.75 mm.

Bacterial cultures and antibiotic concentration. After [^{18}F]FDG PET and pQCT imaging, the animals were killed at 6 weeks by the intravenous administration of sodium pentobarbital (Mebunat; Orion Oyj). By using sterile techniques, the bone defect area was exposed and swab specimens for culture were taken both from the bone defect itself and from the surrounding area of soft tissues in order to confirm the presence of persistent staphylococcal bone infection. The specimens were cultured for 20 h at 35°C on blood agar plates.

The ciprofloxacin concentration was measured at two locations of the bone. The first sample was taken from the metaphyseal bone proximal to the site of implantation of the composite material. The second sample was taken from the cortical bone starting 5 mm distally from the distal edge of the defect. The bone samples were cut with a high-speed blade under continuous saline irrigation for cooling and washing out of blood contamination. For comparison, one additional animal was used to evaluate the concentrations of ciprofloxacin in the local bone tissue and systemic serum after normal intravenous administration. The animal received a 60-min intravenous infusion (10 mg/kg) of ciprofloxacin (Ciproxin; Bayer AG, Leverkusen, Germany). The serum sample and bone tissue specimens were obtained 120 min after the start of the ciprofloxacin infusion.

A high-performance liquid chromatographic (HPLC) method with fluorescence detection (FLD) and internal standard method (CRST Bioanalytics, Turku, Finland) was applied for determination of the concentrations of ciprofloxacin in bone and serum. Ofloxacin was used as an internal standard. The bone specimens were ground with a homogenizer (Mikro-Dismembrator S; B. Brown, Melsungen, Germany). Finely ground bone (100 to 300 mg) was weighed and mixed with internal standard solution (1.0 μg/ml in methanol), methanol, water, and perchloric acid in water. The suspension was centrifuged, and the supernatant was filtered through a 0.45-μm-pore-size membrane filter. Finally, 20 μl of the sample was injected into the HPLC column. Standard samples and quality control samples were handled identically, but instead of methanol, certain amounts of solutions containing ciprofloxacin in methanol and methanol were added. The frozen serum sample was thawed in a refrigerator, and 0.5 ml of serum was mixed with perchloric acid and the internal standard. After centrifugation, the supernatant was transferred into an autosampler vial, from which 20 μl was injected into the HPLC column. HPLC-FLD analysis was carried out with a Waters 2695 separations module, a Waters 2475 multi λ fluorescence detector, and Millennium (version 4.0) software. A Nova-Pak C_8 column (150 by 3.9 mm [inner diameter, 60 Å]; Waters Co., Milford, Mass.) was used to separate the ciprofloxacin. The mobile phase consisted of 9% acetonitrile and 91% buffer. The buffer was filtered before use through a 0.45-μm-pore-size HV filter (Millipore Corporation, Bedford, Mass.). The flow rate of the mobile phase was 1.0 ml/min. The excitation wavelength was 290 nm, and the emission wavelength was 470 nm. A standard curve was generated by using weighted ($1/x$) linear regression. The measured concentration of ciprofloxacin was expressed per weight of bone tissue (micrograms per gram). The measured concentration of ciprofloxacin in serum was expressed in micrograms per milliliter.

Radiography and histomorphometry. After the specimens for culture were obtained, the specimens were subjected to radiography with an Alpha RT mammography device (Instrumentarium Corp., Tuusula, Finland). The radiographic presence of osteomyelitic bone changes was graded on a scale of increasing severity from 0 to 4 according to the osteomyelitis system of Mader and Wilson (24).

For the histomorphometric analysis, the bone blocks containing the defect area were fixed in 70% ethanol, dehydrated in a graded series of ethanol, cleared in xylene, and embedded in isobornylmethacrylate (Technovit 1200 VLC; Kulzer, Wehrheim, Germany). The specimens were cut in the cross-sectional plane at the center of the cortical window by using a water-cooled, high-speed, low-feed saw equipped with a diamond-impregnated blade. Sections of 20 μm were prepared by a cutting-and-grinding technique (Exakt Apparatebau, Hamburg, Germany) and were stained by a modified van Gieson staining method. The amount of new bone formation was measured from the area estimated to represent the original medullary cavity by using a computerized image analysis system (Micro-Scale TC; Digithurst Ltd., Royston, England) and was expressed as the percentage of the cross-sectional medullary area outside the composite. In addition, the sections were analyzed for the amount of new bone within the cortical defect, expressed as the percentage of the original defect area.

SEM. The bone blocks were also analyzed by backscattered electron imaging (BEI) of scanning electron microscopy (SEM) images (BEI-SEM analysis). The images were used to study the osteoconductivity of the composite material. Before the BEI-SEM analysis, the bone blocks were carbon coated by use of a JEE-4X vacuum evaporator (JEOL Ltd., Tokyo, Japan). The analysis was performed with a scanning electron microscope (XL-30; Philips, Eindhoven, The Netherlands) equipped with a backscattered electron detector for imaging and an energy dispersive spectrometer (model DX-4; EDAX International, Mahwah, N.J.) for elemental analysis.

Statistical analyses. The primary end point of this study was to show that the [^{18}F]FDG uptake, as determined by PET, was lower in the treated-infection group than in the untreated-infection group. To perform a power analysis, we expected a difference of 2.0 in the SUV ratio between the treated-infection group and the untreated-infection group. An SD in the SUV ratio of 1.0 was expected for both groups. By using analysis of variance (ANOVA) with four groups, a type I error of 0.05, and a power of 80%, seven animals was needed to detect a statistically significant difference between the two groups. The significance of the differences observed in [^{18}F]FDG PET and pQCT imaging and histomorphometric analysis between the treated-infection group and the control groups was calculated by a one-way ANOVA with the post-hoc Tukey test. The results of the radiographic scores were analyzed by Kruskall-Wallis ANOVA with Dunn's post-hoc test. A P value of 0.05 was considered significant. All statistical analyses were conducted by using SPSS statistical software (version 11.5; SPSS Inc., Chicago, Ill.).

RESULTS

All groups of animals in which osteomyelitis was induced experienced a temporary loss of body weight and also showed clinical signs of mild local infection. Only the negative control group showed an increase in body weight 3 and 6 weeks after the debridement surgery. Only a single control animal with the infected medullary space filled with BaG microspheres developed a major local infection and was euthanized 5 weeks after the debridement surgery.

Bacterial cultures. At the time of surgical debridement (2 weeks after implantation of bone cement with *S. aureus* inoculation) but before the start of treatment for the infection, the inoculated pathogen was isolated from swab specimen cultures and from cultures of bone cement removed from all except one of the animals ($n = 23$). None of the animals in the negative control group ($n = 8$) had positive bacterial cultures.

At the time that the animals were killed (6 weeks after debridement and the start of treatment for the infection), all the animals in the sham-treated and untreated-infection groups had culture-positive *S. aureus* deep bone infections. In addition, culture-positive soft tissue infections were found in three of eight animals in the untreated-infection group and in three of five animals in the sham-treated group. Among the animals in the treated-infection group, all cultures of bone were negative at the time that the animals were killed. However, three animals had culture-positive soft tissue infections. At the time that the animals in the negative control group were killed, cultures of bone and soft tissues from all the animals were negative for the bacteria.

[^{18}F]FDG PET imaging. There were significant differences in [^{18}F]FDG uptake between the experimental and the control groups. Treatment with AB-PDLLA-BaG significantly decreased the levels of [^{18}F]FDG uptake at 6 weeks, when the level of uptake in the treatment group was approaching that for the negative control group (Fig. 1). At 6 weeks, the treated-infection group showed a significantly lower SUV ratio than the sham-treated and the untreated-infection groups ($P = 0.006$ and $P = 0.001$, respectively). The differences between the groups at 3 and 6 weeks were similar, when [^{18}F]FDG uptake was expressed as the SUVs. The mean SUVs for the treated-infection group were 1.37 (SD, 0.79) at 3 weeks and 0.63 (SD, 0.18) at 6 weeks. The corresponding SUVs for the untreated-infection group were 1.95 (SD 0.71) at 3 weeks and 1.69 (SD 0.85) at 6 weeks.

pQCT. On the basis of sequential pQCT imaging, the cortical windows were open in all animals at 3 weeks. At 6 weeks, there was a significant difference in the extent of cortical defect healing (Fig. 2). On average, the cortical defect was closed by 89% of its original length in the treated-infection group and 77% in the negative control group. The corresponding values for the untreated-infection and sham-treated groups were 34 and 7%, respectively, which differed significantly from those for the negative control group ($P = 0.007$ and $P < 0.001$, respectively).

At the level of the cortical defect, the pQCT analysis revealed significant differences in the density of the content of the medullary cavity (Fig. 3), which represents the sum of the effects of the endosteal new bone formation and the implant material. The negative control group had low density values

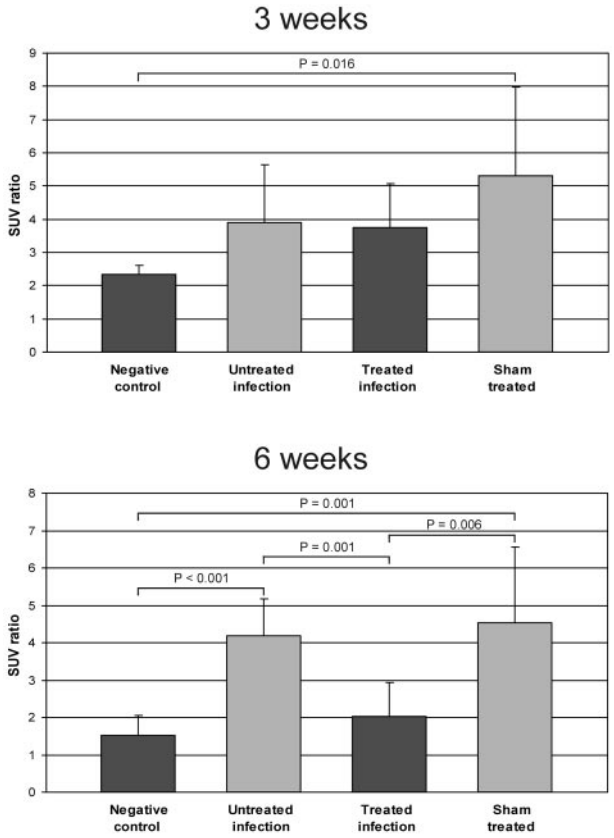

FIG. 1. [^{18}F-FDG] PET imaging at 3 and 6 weeks. The bars represent the mean SUV ratios ± SD (n = 5 to 9). Treatment with AB-PDLLA-BaG significantly decreased the level of [^{18}F]FDG uptake compared with those for the untreated-infection group and the sham-treated infection group at 6 weeks.

compared with those of all other groups. Reflecting the infection-induced reactive new bone formation, the medullary canals of the tibias in the untreated-infection group showed increased densities (P = 0.003 at 3 weeks; P = 0.036 at 6 weeks) compared with those in the negative control group. The two groups with implanted composite material (the treated-infection and sham-treated groups) showed high density values with minimal time-related changes.

Radiography, histomorphometry, and BEI-SEM. In the untreated-infection and sham-treated groups, plain radiographs showed localized osteomyelitis with moderate bone destruction. Similar changes were not observed in the animals in the treated-infection and the negative control groups. By using the osteomyelitis scoring system of Mader and Wilson (24), the mean scores were similar for the treated-infection and the negative control groups (0.4 ± 0.52 and 0.25 ± 0.46, respectively). The corresponding scores were 3.4 ± 0.46 and 3.8 ± 0.45 for the untreated-infection group and sham-treated group, respectively, which differed significantly from those for the negative control group (P = 0.001 for both comparisons).

Histological specimens showed distinct differences in the light-microscopic appearance of the bone medullary space between the experimental and the control animals. In the treated-infection group, the blocks of the composite material with BaG microspheres were surrounded by new bone starting

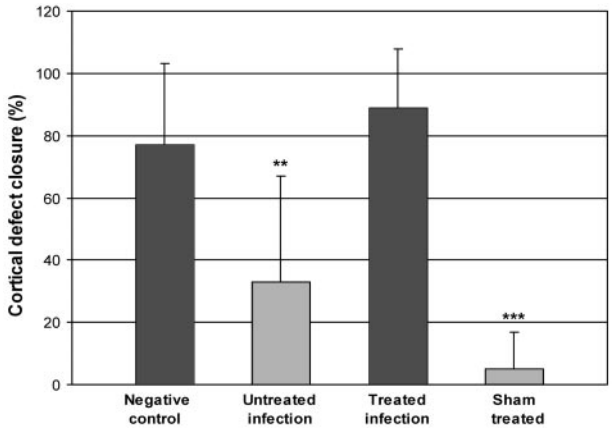

FIG. 2. Cortical defect healing evaluated at 6 weeks. The bars represent the defect closure expressed as the mean ± SD (n = 5 to 9) percentage of the original defect length based on pQCT measurements. Healing of the cortical defect was significantly delayed in the untreated-infection and sham-treated groups compared with that in the negative control group (**, P = 0.007; ***, $P < 0.001$).

mainly from the endosteal surface of the tibia. The composite material was already partially biodegraded in these animals, especially in the central areas of the canal. In contrast, in the sham-treated group, the composite material was still present in the canal and the amount of surrounding new bone was minimal. The infected control animal in which the canal was filled only with BaG showed extensive new bone formation around the BaG microspheres. The surfaces of the BaG microspheres showed two reaction layers, with intimate contact with surrounding new bone as an indication of biomaterial-related osteoconductivity. A corresponding finding of the BaG response was observed by BEI-SEM analysis of tissue specimens from the treated-infection group (Fig. 4). BEI-SEM analysis confirmed the osteoconductivity of the composite material by showing trabeculae of new bone in direct contact with the BaG microspheres (Fig. 4).

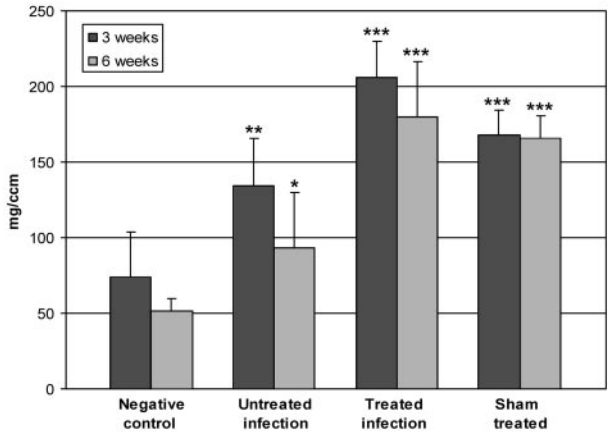

FIG. 3. pQCT density of the medullary cavity at the defect area at 3 and 6 weeks. The bars represent the mean pQCT density values ± SD (n = 5 to 9), expressed as milligrams per cubic centimeter. The densities for the untreated-infection group, the treated-infection group and the sham-treated group differed significantly (*, $P < 0.05$; **, $P < 0.01$; ***, $P < 0.001$) from those for the negative control group.

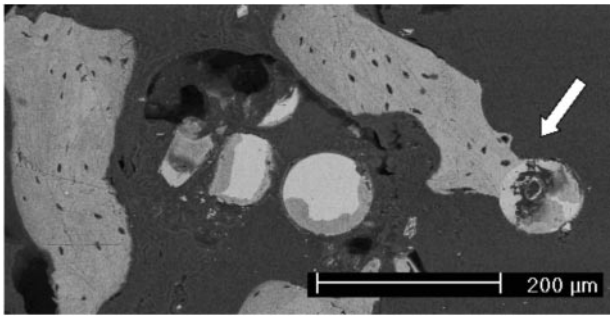

FIG. 4. BEI-SEM micrograph demonstrating new bone formation in intimate contact with a BaG microsphere (white arrow) in the treated-infection group. Magnification, ×100.

At the level of the cortical defect, the findings for the histological specimens corroborated the results of the pQCT analyses. The cortical defects in the negative control group were healing uneventfully with a solid bridge of new bone (Fig. 5A). As a sign of a continuing infection process, the untreated-infection group showed widespread reactive new bone formation both endosteally and periosteally next to the defect area (Fig. 5B). The treated-infection group showed a healing process consisting of a defect union with new bone, similar to the negative control group (Fig. 5C). The cortical defect in the sham-treated group showed a completely different appearance. The defects were open, and there were signs of expulsion of the nondegraded composite material from the medullary canal into the defect opening (Fig. 5D).

In the histomorphometric analysis, the amount of intramedullary new bone was significantly higher in the treated-infection group than in the negative control group ($P = 0.045$) (Fig. 6). The untreated-infection and sham-treated groups also showed a trend for an increased amount of new intramedullary bone, but the differences compared with the amounts for the negative control group were not statistically significant.

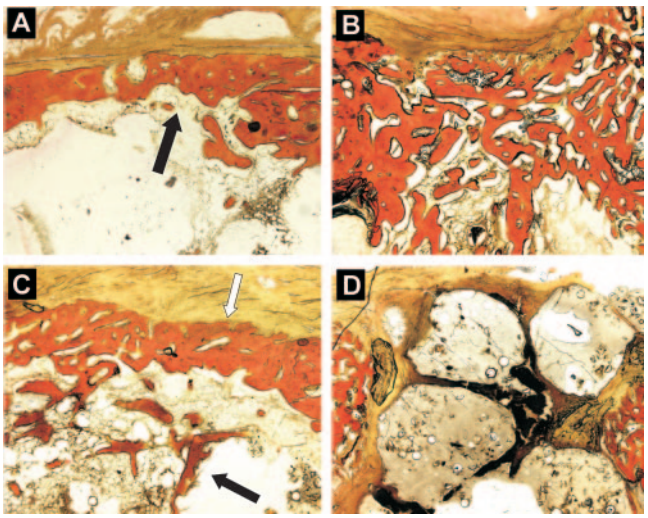

FIG. 5. Histological sections demonstrating the healing of cortical bone. (A) Healed cortical window (black arrow) in negative control group; (B) extensive reactive new bone formation in cortical defect of untreated-infection group; (C) healed cortical window (white arrow) and associated intramedullary new bone formation (black arrow) in treated-infection group; (D) unhealed cortical defect with extruding biomaterial fillers in sham-treated group. Modified van Gieson stain. Magnification, ×25.

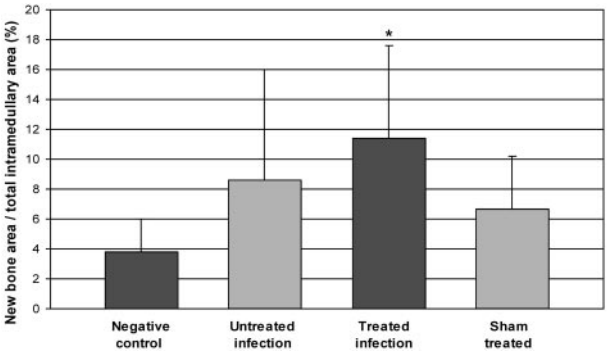

FIG. 6. The amount of intramedullary new bone measured by histomorphometry. The bars represent the mean areas of new bone ± SD ($n = 5$ to 9) expressed as the percentage of the cross-sectional area of the medullary canal. Treatment with AB-PDLLA-BaG resulted in significantly (*, $P < 0.05$) increased new intramedullary bone formation compared with that in the negative control group.

Antibiotic concentration. In the treated-infection group, local antibiotic therapy resulted in a relatively high concentration of ciprofloxacin in bone. The mean concentrations of ciprofloxacin were 12.6 μg/g (median, 2.1 μg/g; SD, 20.6 μg/g; $n = 9$) in the proximal bone samples and 1.4 μg/g (median, 1.2 μg/g; SD, 0.7 μg/g; $n = 9$) in the distal bone samples. In the control animal that received a therapeutic (10 mg/kg) dose of ciprofloxacin intravenously, the concentration of ciprofloxacin measured in serum was 2.2 μg/ml at 120 min, and the corresponding concentrations of ciprofloxacin in bone tissue were lower in both the proximal region (0.8 μg/g) and the distal region (0.6 μg/g) compared with those obtained by local antibiotic therapy.

DISCUSSION

Despite continuous advances in the surgical and antimicrobial armamentarium, the treatment of bone infections remains a challenge even in specialized centers with a team approach involving clinicians in different subspecialities. The local delivery of antibiotics by using biodegradable materials is a promising treatment modality which offers several benefits over present therapies.

This study evaluated the efficacy of a ciprofloxacin-releasing bioabsorbable osteoconductive material for the treatment of experimental *S. aureus* osteomyelitis. As a novel noninvasive imaging modality, [^{18}F]FDG PET was applied to monitor the treatment response quantitatively. [^{18}F]FDG PET is able to image activated granulocytes and mononuclear cells (37). On the basis of the results of the microbiological analyses, the local treatment was highly successful for eradication of the *S. aureus* pathogen from bone. Six weeks after the start of therapy, there was no significant difference in the levels of [^{18}F]FDG uptake between the treated-infection group and the negative control group. The local therapy resulted in adequate concentrations of ciprofloxacin in bone tissue without any harmful effects on bone healing. BaG microspheres, as the osteopromotive component of the composite, were used to provide an osteoconductive surface for the growth of new bone. Such an effect

would reduce the need for bone grafting after the resolution of infection and at the time of composite degradation. However, we need to perform a long-term follow-up of the osteoconductive response in order to make any definitive conclusions. While the treatment was successful for eradication of the bone pathogen, soft tissue infections were seen in three animals, confirming that there is still a need for systemic antimicrobial treatment in addition to local therapy for a certain time period.

The polylactide (PDLLA) was selected to act as a carrier because it undergoes gradual degradation in a controlled manner and dissolves at physiological pH. Several previous in vitro and in vivo studies (1, 6, 17, 25, 28, 30, 32, 39) have delineated the use of polymers in different chemistries (polylactides, copolymers of lactide and glycolide, polyanhydrides, and polycaprolactone) as systems for the delivery of various antibiotics. The same composites have uniformly given positive results for the treatment of experimental osteomyelitis (2, 8, 16, 19, 29, 34, 38). Previous studies have mainly focused on antibiotic release from polymer composites during a course of only 1 to 3 months, which is less than the desired optimum for the therapy of treatment-resistant bone infections. Extending the results of the previous studies, the present study evaluated the efficacy of a polymer composite with optimized properties for local antimicrobial therapy. On the basis of findings from in vitro studies (Koort et al., unpublished), the composite used results in a long-term release (up to 300 days) of the selected antibiotic (ciprofloxacin) at the therapeutic level (>2 μg/ml) without exceeding the level of 20 μg/ml, and in vivo the serum ciprofloxacin concentration remains below the resolution of the HPLC-FLD method (<5.0 ng/ml). Fluoroquinolones have long been considered the drugs of choice for the treatment of chronic osteomyelitis because of their favorable penetration into poorly vascularized sites of infection, their advantageous bactericidal effects against all probable pathogens of chronic osteomyelitis, and the lack of serious adverse reactions (18, 23). Similar to many antibiotics commonly used for the treatment of bone infections, such as rifampin and gentamicin (12, 13), quinolones may have inhibitory effects on osteoblastic functions at high concentrations (10) and may delay bone healing (31).

Substitute bone materials, such as apatite-wollastonite glass ceramic blocks and hydroxyapatite blocks, have previously been tested to determine whether they act as carriers of antibiotics (15, 20). The use of such materials may result in technical difficulties in controlling the sustained long-term release of the antibiotic. The concept has even been applied in clinical trials of osteomyelitis by use of antibiotic-impregnated calcium phosphate (26). The present study was aimed to test the concept of the use of multifunctional composites for the local treatment of bone infections. The osteoconductive component in the composite applied here did not serve as a carrier of the antibiotic (dissimilar to previous studies) but was used as a self-governing component with a specific mode of action, i.e., the promotion of new bone formation after eradication of the infection. BaGs, a group of synthetic silica-based biomaterials, have several unique properties that favor their use as the osteoconductive component (9, 14). The bioactivity of a glass is based on the formation of silica-rich and hydroxyapatite layers on its surface. Eventually, the reaction layers of the glass bulk form direct chemical bonds with the new bone growing on the glass. Clinically, it is important that the resorption rate of a BaG be able to be modified by changing its composition. A subgroup of BaGs may even have antibacterial properties (36). The present study showed that BaG microspheres can be mixed with a polymer matrix and that the material does not loose its capacity to form direct bonds with new bone.

There were marked differences in the concentrations of ciprofloxacin in the proximal bone samples. Most likely, some of the specimens with unusually high antibiotic concentrations represented tissues which had been in contact with the composite. The distal bone samples, which represented the tissue area 5 mm distally from the edge of the implantation area, had more consistent concentrations of ciprofloxacin.

The present study design had certain limitations. An additional experimental group of animals that received combined local and short-term systemic antimicrobial treatment would have served as a group in which the pathogen was completely eradicated from both bone and soft tissues. For comparison, a group of animals that received systemic antimicrobial treatment alone for the whole 6-week treatment period would also have given a reference for efficacy in comparison with that of traditional systemic treatment. In the microbiological methodology, quantitative cultures of pulverized bone were not performed due to the limited amount of tissue available for the different analyses. However, the strong corroboration between the results of the bacteriological analyses and the [^{18}F]FDG PET studies supports the use of swab cultures as a reliable means of detection of viable bacteria. Although [^{18}F]FDG PET seems to be a highly accurate imaging modality for the diagnosis of chronic musculoskeletal infections (5, 21), there is still a need for bacterium-specific infection-imaging agents for PET. Recently, the promising labeled compound ^{18}F-labeled ciprofloxacin failed to be a bacterium-specific infection tracer (22).

In conclusion, this experimental study shows that a new drug delivery system based on controlled, long-acting ciprofloxacin release from a poly(DL) lactic acid matrix is efficient for the treatment of localized osteomyelitis due to *S. aureus*. The bioabsorbable multifunctional composite applied included an osteoconductive component (BaG microspheres). This type of bone defect filler with antimicrobial properties could restore the bone stock after successful eradication of the infection.

ACKNOWLEDGMENTS

J.K.K. and T.J.M. are Ph.D. students supported by the Finnish Graduate School for Musculoskeletal Diseases. This work was financially supported by the National Technology Agency of Finland (TEKES).

We are grateful to Pentti Huovinen for advice on the design of the study. We acknowledge Tero Vahlberg for consultation on the statistical analysis.

REFERENCES

1. **Ambrose, C. G., G. R. Gogola, T. A. Clyburn, A. K. Raymond, A. S. Peng, and A. G. Mikos.** 2003. Antibiotic microspheres: preliminary testing for potential treatment for osteomyelitis. Clin. Orthop. **415:**279–285.
2. **Calhoun, J. H., and J. T. Mader.** 1997. Treatment of osteomyelitis with a biodegradable antibiotic implant. Clin. Orthop. **341:**206–214.
3. **Cierny, G., J. T. Mader, and J. J. Penninck.** 2003. A clinical staging system for adult osteomyelitis. Clin. Orthop. **414:**7–24.
4. **DeGrado, T. R., T. G. Turkington, J. J. Williams, C. W. Stearns, J. M. Hoffman, and R. E. Coleman.** 1994. Performance characteristics of a whole-body PET scanner. J. Nucl. Med. **35:**1398–1406.
5. **De Winter, F., C. van de Wiele, D. Vogelaers, K. de Smet, R. Verdonk, and**

R. A. Dierckx. 2001. Fluorine-18 fluorodeoxyglucose-positron emission tomography: a highly accurate imaging modality for the diagnosis of chronic musculoskeletal infections. J. Bone Joint Surg. **83A:**651–660.
6. **Dounis, E., T. Korakis, A. Anastasiadis, K. Kanellakopoulou, A. Andreopoulos, and H. Giamarellou.** 1996. Sustained release of fleroxacin *in vitro* from lactid acid polymer. Bull. Hosp. Joint Dis. **55:**16–19.
7. **Fitzgerald, R. H., Jr.** 1983. Experimental osteomyelitis: description of a canine model and the role of depot administration of antibiotics in the prevention and treatment of sepsis. J. Bone Joint Surg. **65A:**371–380.
8. **Garvin, K. L., J. A. Miyano, D. Robinson, D. Giger, J. Novak, and S. Radio.** 1994. Polylactide/polyglycolide antibiotic implants in the treatment of osteomyelitis. J. Bone Joint Surg. **76A:**1500–1506.
9. **Hench, L. L.** 1988. Bioactive ceramics. Ann. N. Y. Acad. Sci. **523:**54–71.
10. **Holtom, P. D., S. A. Pavkovic, P. D. Bravos, M. J. Patzakis, L. E. Shepherd, and B. Frenkel.** 2000. Inhibitory effects of the quinolone antibiotics trovafloxacin, ciprofloxacin, and levofloxacin on osteoblastic cells *in vitro*. J. Orthop. Res. **18:**721–727.
11. **Holtom, P. D., and M. J. Patzakis.** 2003. Newer methods of antimicrobial delivery for bone and joint infections. Instr. Course Lect. **52:**745–749.
12. **Isefuku, S., C. J. Joyner, and A. H. Simpson.** 2001. Toxic effect of rifampicin on human osteoblast-like cells. J. Orthop. Res. **19:**950–954.
13. **Isefuku, S., C. J. Joyner, and A. H. Simpson.** 2003. Gentamicin may have an adverse effect on osteogenesis. J. Orthop. Trauma **17:**212–216.
14. **Itälä, A., V. V. Välimäki, R. Kiviranta, H. O. Ylänen, M. Hupa, E. Vuorio, and H. T. Aro.** 2003. Molecular biologic comparison on new bone formation and resorption on microrough and smooth bioactive glass microspheres. J. Biomed. Mater. Res. **B65:**163–170.
15. **Itokazu, M., T. Ohno, T. Tanemori, E. Wada, N. Kato, and K. Watanabe.** 1997. Antibiotic-loaded hydroxyapatite blocks in the treatment of experimental osteomyelitis in rats. J. Med. Microbiol. **46:**779–783.
16. **Jakob, E., J. A. Setterstrom, D. E. Bach, J. R. Heath III, L. M. McNiesh, and G. Cierny III.** 1991. Evaluation of biodegradable ampicillin anhydrate microcapsules for local treatment of experimental staphylococcal osteomyelitis. Clin. Orthop. **267:**237–244.
17. **Kanellakopoulou, K., M. Kolia, A. Anastassiadis, T. Korakis, E. J. Giamarellos-Bourboulis, A. Andreopoulos, E. Dounis, and H. Giamerellou.** 1999. Lactic acid polymers as biodegradable carriers of fluoroquinolones: an in vitro study. Antimicrob. Agents Chemother. **43:**714–716.
18. **Kanellakopoulou, K., and E. J. Giamarellos-Bourboulis.** 2000. Carrier systems for the local delivery of antibiotics in bone infections. Drugs **59:**1223–1232.
19. **Kanellakopoulou, K., N. Galanakis, E. J. Giamarellos-Bourboulis, C. Rifiotis, K. Papakostas, A. Andreopoulos, E. Dounis, P. Karagianakos, and H. Giamarellou.** 2000. Treatment of experimental osteomyelitis caused by methicillin-resistant *Staphylococcus aureus* with a biodegradable system of lactic acid polymer releasing pefloxacin. J. Antimicrob. Chemother. **46:**311–314.
20. **Kawanabe, K., Y. Okada, Y. Matsusue, H. Iida, and T. Nakamura.** 1998. Treatment of osteomyelitis with antibiotic-soaked porous glass ceramic. J. Bone Joint Surg. Br. **80:**527–530.
21. **Koort, J. K., T. J. Mäkinen, J. Knuuti, J. Jalava, and H. T. Aro.** 2004. Comparative ^{18}F-FDG-PET imaging of experimental *Staphylococcus aureus* osteomyelitis and normal bone healing. J. Nucl. Med. **45:**1406–1411.
22. **Langer, O., M. Brunner, M. Zeitlinger, S. Ziegler, U. Müller, G. Dobrozemsky, E. Lackner, C. Joukhadar, M. Mitterhauser, W. Wadsak, E. Minar, R. Dudczak, K. Kletter, and M. Müller.** 2005. In vitro and in vivo evaluation of [^{18}F]ciprofloxacin for the imaging of bacterial infections with PET. Eur. J. Nucl. Med. Mol. Imaging **32:**143–150.
23. **Lew, D. P., and F. A. Waldvogel.** 1995. Quinolones and osteomyelitis: state-of-the-art. Drugs **49**(Suppl. 2)**:**101–111.
24. **Mader, J. T., and K. J. Wilson.** 1983. Comparative evaluation of cefamandole and cephalothin in the treatment of experimental *Staphylococcus aureus* osteomyelitis in rabbits. J. Bone Joint Surg. **65A:**507–513.
25. **Mader, J. T., J. Calhoun, and J. Cobos.** 1997. In vitro evaluation of antibiotic diffusion from antibiotic-impregnated biodegradable beads and polymethylmethacrylate beads. Antimicrob. Agents Chemother. **41:**415–418.
26. **McKee, M. D., L. M. Wild, E. H. Schemitsch, and J. P. Waddell.** 2002. The use of an antibiotic-impregnated, osteoconductive, bioabsorbable bone substitute in the treatment of infected long bone defects: early results of a prospective trial. J. Orthop. Trauma **16:**622–627.
27. **Miclau, T., M. L. Edin, G. E. Lester, R. W. Lindsey, and L. E. Dahners.** 1998. Effect of ciprofloxacin on the proliferation of osteoblast-like MG-63 human osteosarcoma cells in vitro. J. Orthop. Res. **16:**509–512.
28. **Nie, L., D. P. Nicolau, C. H. Nightingale, B. D. Browner, and R. Quintiliani.** 1995. *In vitro* elution of ofloxacin from a bioabsorbable polymer. Acta Orthop. Scand. **66:**365–368.
29. **Nie, L., D. P. Nicolau, P. R. Tessier, H. P. Kourea, B. D. Browner, and C. H. Nightingale.** 1998. Use of a bioabsorbable polymer for the delivery of ofloxacin during experimental osteomyelitis treatment. J. Orthop. Res. **16:**76–79.
30. **Overbeck, J. P., S. T. Winckler, R. Meffert, P. Törmälä, H. U. Spiegel, and E. Brug.** 1995. Penetration of ciprofloxacin into bone: a new bioabsorbable implant. J. Investig. Surg. **8:**155–162.
31. **Perry, A. C., B. Prpa, M. S. Rouse, K. E. Piper, A. D. Hanssen, J. M. Steckelberg, and R. Patel.** 2003. Levofloxacin and trovafloxacin inhibition of experimental fracture-healing. Clin. Orthop. **414:**95–100.
32. **Ramchandani, M., and D. Robinson.** 1998. *In vitro* and *in vivo* release of ciprofloxacin from PLGA 50:50 implants. J. Control. Release **54:**167–175.
33. **Rissing, J. P.** 1990. Animal models of osteomyelitis. Knowledge, hypothesis, and speculation. Infect. Dis. Clin. N. Am. **4:**377–390.
34. **Rutledge, B., D. Huyette, D. Day, and J. Anglen.** 2003. Treatment of osteomyelitis with local antibiotics delivered via bioabsorbable polymer. Clin. Orthop. **411:**280–287.
35. **Shuford, J. A., and J. M. Steckelberg.** 2003. Role of oral antimicrobial therapy in the management of osteomyelitis. Curr. Opin. Infect. Dis. **16:**515–519.
36. **Stoor, P., E. Soderling, and R. Grenman.** 1999. Interactions between the bioactive glass S53P4 and the atrophic rhinitis-associated microorganism *Klebsiella ozaenae*. J. Biomed. Mater. Res. **48:**869–874.
37. **Sugawara, Y., T. D. Gutowski, S. J. Fisher, R. S. Brown, and R. L. Wahl.** 1999. Uptake of positron emission tomography tracers in experimental bacterial infections: a comparative biodistribution study of radiolabeled FDG, thymidine, L-methionine, ^{67}Ga-citrate, and ^{125}I-HSA. Eur. J. Nucl. Med. **26:**333–341.
38. **Wei, G., Y. Kotoura, M. Oka, T. Yamamuro, R. Wada, S. Hyon, and Y. Ikada.** 1991. A bioabsorbable delivery system for antibiotic treatment of osteomyelitis. The use of lactic acid oligomer as a carrier. J. Bone Joint Surg. Br. **73:**246–252.
39. **Zhang, X., U. P. Wyss, D. Pichora, and M. P. Goosen.** 1994. Biodegradable controlled antibiotic release devices for osteomyelitis: optimization of release properties. J. Pharm. Pharmacol. **46:**718–724.
40. **Ziran, B. H., N. Rao, and R. A. Hall.** 2003. A dedicated team approach enhances outcomes of osteomyelitis treatment. Clin. Orthop. **414:**31–36.